

Cooling and Localization Dynamics in Optical Lattices

G. Raithel, G. Birkl,* A. Kastberg,† W. D. Phillips, and S. L. Rolston

National Institute of Standards and Technology, PHYS A167, Gaithersburg, Maryland 20899

(Received 12 August 1996)

Using Bragg scattering as a sensitive probe, we study how atoms are cooled and localized after the sudden turn-on of 1D and 3D optical lattices. We measure the time evolution of the mean-square position spread of the atoms in the lattice potential wells, a quantity proportional to their effective temperature. The rate of exponential approach to equilibrium is proportional to the photon scattering rate and about 6 times faster in 1D than in 3D. This simple proportionality was unexpected, based on the usual model of Sisyphus cooling, but is in agreement with our 1D Monte Carlo simulations. [S0031-9007(96)02228-4]

PACS numbers: 32.80.Lg, 32.80.Pj, 42.50.Vk

Optical lattices are periodic light-shift potentials for atoms, created by the interference of multiple laser beams. Atoms can be laser cooled and localized at the potential minima [1–3]. Recently, Bragg scattering of a weak probe was introduced as a new tool to study atoms in optical lattices [4,5]. The intensity of the Bragg scattered light is exponentially dependent on the mean square of the position spread of the atoms in the potential wells. This along with the high time resolution provides a new way to investigate the motion of atoms in optical lattices. Results based on this technique fill a gap in a field where most experimental and theoretical studies have dealt with steady-state properties but only a few with the time dependence of atomic motion [6,7]. In this work we employ Bragg scattering to investigate experimentally for the first time how atoms in an optical lattice approach their steady state. Since we cool cesium on the $6S_{1/2}, F = 4 \rightarrow 6P_{3/2}, F' = 5$ transition, we explore polarization gradient (Sisyphus) cooling for large angular momenta, where there are multiple potentials capable of trapping the atoms at the same location. We find that the cooling rate is proportional to intensity, in agreement with our Monte Carlo calculations, but in direct contradiction with the simple Sisyphus model of laser cooling [8], which nonetheless correctly predicts the linear dependence of temperature on intensity.

We investigate the 1D $\text{lin}\perp\text{lin}$ lattice configuration (counterpropagating beams with orthogonal polarizations) [1–3] as well as its 3D generalization consisting of two pairs of linearly polarized laser beams configured as in Ref. [4]. The lattices are operated close to resonance ($\lambda = 852$ nm, $\Gamma/2\pi = 5.2$ MHz). In both 1D and 3D we choose the quantization axis z to be orthogonal to the polarization vectors of the lattice beams. In 1D, the light field displays alternating pure σ^+ and σ^- polarization in planes perpendicular to z , spaced by $\lambda/4$. In 3D, there are points of pure σ^+ and σ^- polarization forming a centered tetragonal lattice with a spacing of $\lambda/2\sqrt{2}$ along z , and $\lambda/\sqrt{2}$ along x and y . As the atoms are cooled and localized around the lattice sites of σ^\pm polarization, they form equidistant, dilutely occupied planes of atoms. The mean-square position spread of the atoms about the lattice

sites can be deduced from the Bragg reflectivity, except for an additive constant.

Consider our 1D lattice, a σ^+ -polarized probe beam and a detection apparatus sensitive to σ^+ -polarized light. When saturation and higher order reflections can be neglected, the detected Bragg intensity from a single atom with a wave function $|\psi\rangle$ distributed throughout the lattice [9] is proportional to

$$I_B \sim |\langle\psi|e^{i\mathbf{K}\cdot\mathbf{r}}V_B V_P|\psi\rangle|^2, \quad (1)$$

where the wave function consists of subcomponents according to the magnetic sublevels of cesium. The operators V_P and V_B describe the electric-dipole coupling between the internal atomic states by the probe wave and the Bragg-reflected wave, respectively. The operator product $V_B V_P$ connects two states in the $F = 4$ manifold through the $F' = 5$ manifold of excited states. The operator $e^{i\mathbf{K}\cdot\mathbf{r}}$ contains the momentum transfer \mathbf{K} associated with Bragg reflection and describes its effect on the atom center-of-mass coordinate. We choose \mathbf{K} such that the average position distribution of the atoms along \mathbf{K} has a periodicity fulfilling the first-order Bragg condition.

A simplification of Eq. (1) is obtained as follows. Our own and other [10] Monte Carlo simulations show that when the lattice is turned on most of the atoms are rapidly pumped into the extreme magnetic sublevels, $m_F = \pm 4$. Thus, we can neglect states other than $m_F = \pm 4$. Because of the strong asymmetry of the Clebsch-Gordan coefficients involved, the operators V_P and V_B mostly couple the states $m_F = 4$ and $m_{F'} = 5$. Then, Eq. (1) becomes approximately

$$I_B \sim |v_B v_P|^2 |\langle\psi_4|e^{i\mathbf{K}\cdot\mathbf{r}}|\psi_4\rangle|^2, \quad (2)$$

where the wave function is restricted to the dominant component, $m_F = 4$, and the operator product $V_B V_P$ is replaced by a single constant $|v_B v_P|$. If we use the approximation of Eq. (2) and assume that the atoms have a Gaussian position distribution around the lattice sites with mean-square spread $\Delta\xi^2$ (ξ being measured along \mathbf{K}), the Bragg reflectivity is proportional to the Debye-Waller factor $\beta = \exp(-K^2\Delta\xi^2)$. Our Monte Carlo simulations

show that calculating the exact Bragg reflectivity with Eq. (1), and then using the Debye-Waller factor to extract $\Delta\xi^2$ yields an excellent approximation to the true mean-square position spread of the atoms, given by the full wave function. We find both experimentally and theoretically that as the atoms cool, the Bragg reflectivity $I_B(t)$ and $\Delta\xi(t)^2$ approach single steady-state values $I_B(\infty)$ and $\Delta\xi^2(\infty)$, for a wide range of parameters.

Experimentally, we determine $\Delta\xi^2(t)$ from

$$\Delta\xi^2(t) = -\frac{\ln[I_B(t)/I_B(\infty)]}{K^2} + \Delta\xi^2(\infty), \quad (3)$$

where for $\sqrt{\Delta\xi^2(\infty)}$ we use the previously observed steady-state values of $\lambda/7.3 \pm 5\%$ (3D) and $\lambda/18 \pm 7\%$ (1D), which were found to be independent of the lattice parameters [2,11]. The 1D value agrees with our Monte Carlo simulations. For $I_B(\infty)$ we use the steady-state value of the Bragg intensity averaged over several runs with different parameters. The extraction of an evolution rate is not influenced by the choice of $I_B(\infty)$ or $\Delta\xi^2(\infty)$. In the approximation of harmonic potential wells, $\Delta\xi^2$ is proportional to the potential energy of the trapped atoms and to their kinetic energy and temperature T . Thus, $\Delta\xi^2(t)$ yields information on how the atoms are cooled.

In our 1D experiment the probe beam is parallel to one of the lattice beams and almost perfectly retroreflected by Bragg scattering (i.e., $\xi = z$), implying a momentum transfer of $K = 2k$ ($k = 2\pi/\lambda$). In 3D the directions of incidence and detection are arranged such that we observe reflection from lattice planes separated by $\lambda/\sqrt{2}$, giving a photon momentum transfer $K = \sqrt{2}k$.

The data are taken in 4 ms cycles [4]. Atoms are collected for 2 ms in a magneto-optical trap, and then cooled for 1 ms in an optical molasses. At this instant, the atoms are presumed to be in a spatially disordered thermal distribution with a temperature of $\approx 10 \mu\text{K}$. This temperature was not measured but was inferred for our $\sigma^+ - \sigma^-$ molasses from the known detuning and intensity following [12]. Approximately $10 \mu\text{s}$ after switching off the molasses beams the lattice beams are suddenly turned on with a rise time $< 0.2 \mu\text{s}$. After a variable atom-lattice interaction time the lattice light is turned off and with a delay of $\approx 0.2 \mu\text{s}$ a weak probe pulse measuring the Bragg reflectivity of the sample is introduced. The width of the probe pulse is only about $0.5 \mu\text{s}$ and its typical intensity 0.1 mW/cm^2 , ensuring that during the probe pulse the Bragg reflectivity does not significantly change due to thermal motion of the atoms or photon recoil. The Bragg-reflected light is detected by a photomultiplier.

Results for $\Delta\xi^2(t)$ obtained from measured 1D and 3D Bragg reflectivities using Eq. (3) are presented in Fig. 1 for different diabatic potential depths U_0 . $U_0 = |\hbar\delta/2| \{ \ln(1+s) - \ln[1 + (1/45)s] \}$ with the saturation parameter $s = 2\Omega^2/(\Gamma^2 + 4\delta^2)$. Ω is the Rabi frequency for the strongest transition at the lattice sites, and δ is the detuning from resonance. For $U_0 > 300$ recoil energies ($E_R = \hbar^2 k^2/2m$), $\Delta\xi^2$ smoothly approaches a

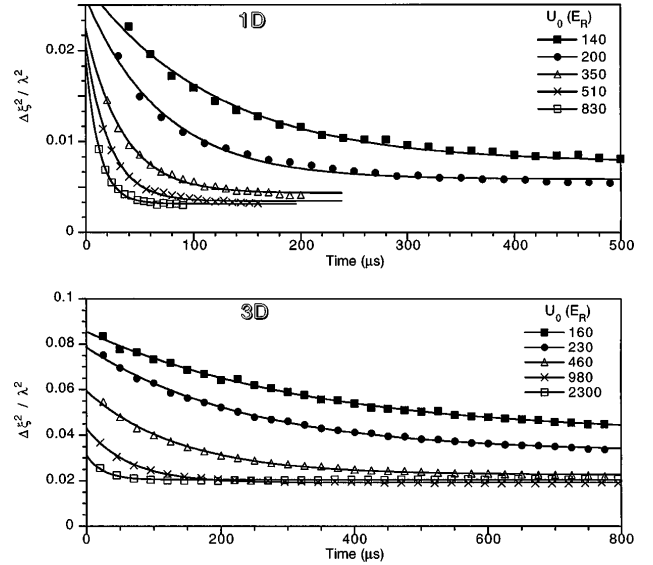


FIG. 1. Mean-square position spread $\Delta\xi^2(t)$ in 1D and 3D as a function of atom-lattice interaction time t for $\delta = -5\Gamma$ and various potential depths U_0 . The probe frequency is 4 MHz below the atomic resonance. The solid lines are exponential fits to the data.

steady-state value, which is nearly independent of U_0 , but different in 1D and 3D. We expect this independence since the shapes of the potentials are self-similar for different depths U_0 and the equilibrium temperature is proportional to U_0 [11].

Figure 1 shows that for constant atom-lattice detuning the approach to steady state is faster for higher U_0 . (The fact that $\Delta\xi^2$ apparently starts from smaller values at higher U_0 reflects initial oscillations in $\Delta\xi^2$ and is addressed below.) After a few μs each data set is well fitted by a single exponential of the form $\Delta\xi^2(t) = [\Delta\xi^2(0) - \Delta\xi^2(\infty)]e^{-t/\tau} + \Delta\xi^2(\infty)$. In order to account for the weak dependence of $\Delta\xi^2(\infty)$ on detuning and intensity, it is treated as a free parameter. The fits yield localization rates τ^{-1} which are plotted versus the potential depth U_0 in Fig. 2. For fixed detuning, the values of τ^{-1} are proportional to U_0 , but for equal potential depths the evolution in 1D is about 6 times faster than in 3D.

We studied the localization rates for different atom-lattice detunings. For each detuning, we observe the proportionality between U_0 and the localization rate for the conditions $s < 0.4$ and $U_0 \geq 300E_R$. The 1D results are shown in Fig. 3 which plots the ratio of the photon scattering rate $\Gamma' = \Gamma s/2(s+1)$ and the localization rate τ^{-1} along with Monte Carlo results (as described below). The ratio $\tau\Gamma'$ is essentially constant, independent of the specific choice of detuning, intensity, and potential depth. We also find this constancy in 3D. In 1D the localization time constant is the time it takes to scatter about 30 photons; 3D requires about 200 photons. If the potential is too shallow or the saturation is too large this number increases.

We investigated the sensitivity of τ to the initial temperature, determined by the parameters of the molasses

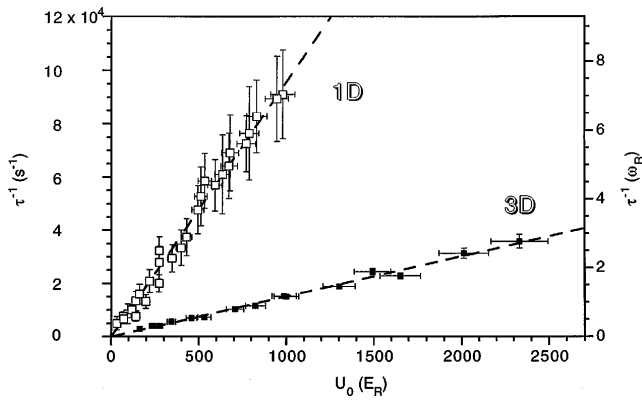


FIG. 2. Localization rate τ^{-1} in s^{-1} and in units of $\omega_R = E_R/\hbar = 2\pi \times 2.07$ kHz versus potential depth U_0 . The dashed lines are linear fits forced through the origin, yielding $\tau^{-1} = 96(U_0/E_R) s^{-1}$ for 1D and $\tau^{-1} = 15.1(U_0/E_R) s^{-1}$ for 3D.

precooling the sample. We observed that τ typically varied by less than 10% when the estimated initial temperature is less than or equal to the steady-state temperature in the lattice. In this, the usual case, the potential energy acquired by the atoms during the sudden onset of the lattice exceeds the kinetic energy in the molasses. For much higher initial temperatures we observe a nonexponential approach to equilibrium with slower evolution at the beginning.

We applied a Monte Carlo wave function method [10,13,14] to simulate our experimental results in 1D for the actual $F = 4 \rightarrow F' = 5$ transition. Reference [10] studied the localization of atoms with a $J = 3 \rightarrow J' = 4$ transition, finding, as we do, the localization rate to be proportional to Γ' . We calculate the average Bragg amplitude using Eq. (1), from typically 50 quantum trajectories and extract $\Delta\xi^2(t)$ via Eq. (3). Then, as in the experiment, exponentials are fitted to $\Delta\xi^2(t)$. In Fig. 4 the localization rates, obtained for $\delta = -5\Gamma$ and -12.5Γ , are plotted versus the potential depth U_0 . As in the experiment, there is a clear linear relationship between the localization rate and U_0 for fixed detuning and it is

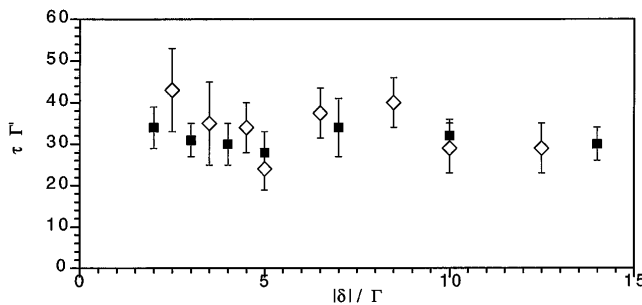


FIG. 3. Ratio of the photon scattering rate Γ' to the localization rate τ^{-1} , as a function of the atom-lattice detuning δ . The squares represent experimental results obtained in 1D; the diamonds are from Monte Carlo simulations. All experimental points are averages of several measurements taken at different lattice intensities.

verified that τ depends only on Γ' . The theoretical rates agree with the experimental ones to within $\approx 20\%$. We consider this to be reasonable agreement, since we have a 10% calibration uncertainty for the lattice intensity, and additional uncertainties due to factors such as nonideal polarizations and slight intensity imbalances between lattice beams. There is also statistical uncertainty of the theoretical value as well as the possibility of a weak influence of the discretization of k space used in the calculations.

We also performed semiclassical Monte Carlo calculations in which the positions and momenta of the atoms are classical variables. The full quantum and the semiclassical results agree within 30%, showing that the semiclassical method gives a fair approximation to the localization and cooling dynamics as well. The moderate deviations mostly occur for $U_0 < 500E_R$ where the semiclassical evolution tends to be slower.

Based on the virial theorem for the harmonic oscillator, we expect a close relationship between the evolution of the kinetic temperature and $\Delta\xi^2(t)$. Our simulations do, in fact, show a close relationship. However, as a result of the anharmonicity of the potential, the ratio between the temperature and localization rates depends on what definition of temperature we use. Our simulations yield a temperature evolution rate in good agreement with the one of $\Delta\xi^2(t)$, when we take the temperature to be proportional to the square of the FWHM of the momentum distribution. If instead we use the mean-square momentum we find evolution rates about 1.5 to 2 times slower due to non-Gaussian wings of the momentum distribution. Nevertheless, whatever definition of temperature we use, we do see the clear relationship of the temperature evolution rate being proportional to the photon scattering rate.

A seminal result of the theory of Sisyphus cooling is that the temperature is proportional to U_0 , originally calculated semiclassically for a $J = 1/2 \rightarrow J = 3/2$ system with the atoms dragged at constant velocity [8]. These calculations show that the cooling rate is *independent* of intensity. We find both experimentally and theoretically for our system that the cooling rate is *proportional* to intensity, even though the temperature dependence is as

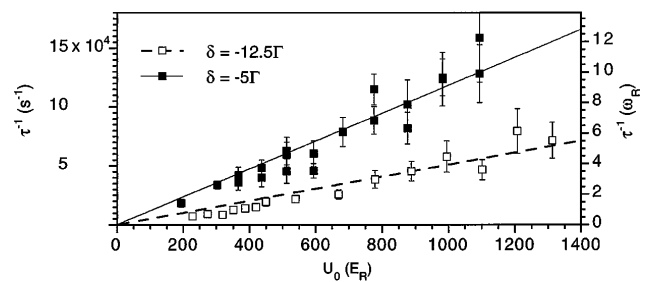


FIG. 4. Localization rate versus the potential depth U_0 calculated by 1D Monte Carlo simulations. The uncertainty estimates are based on separate fits to different parts of the curves $\Delta\xi^2(t)$ and their uncertainties. The linear fits, forced through the origin, yield $\tau^{-1} = 118(U_0/E_R) s^{-1}$ for $\delta = -5\Gamma$, and $\tau^{-1} = 51(U_0/E_R) s^{-1}$ for $\delta = -12.5\Gamma$.

predicted by Sisyphus cooling, implying that the cooling mechanism must be different. While including a finite capture range and a nonlinear friction force may improve the dragged-atom picture, it remains fundamentally unsuitable for trapped atoms. More sophisticated analytical and numerical models for $J = 1/2 \rightarrow J = 3/2$ also fail to reproduce the dependencies we observe [15]. The simple behavior of the temperature and the cooling rate suggests that an analytic model of simplicity and power similar to that of the dragged-atom Sisyphus model should exist for predominantly trapped atoms.

Details of the early-time behavior of the Bragg scattered intensity in 3D are shown in Fig. 5. For high lattice intensities and small detunings, we observe oscillations in $\Delta\xi^2(t)$, the first direct observation of breathing-mode wave packets in optical lattices. Localization builds up rapidly during the first few microseconds and the oscillations are strongly damped due to the anharmonicity of the potential wells [11]. They are induced by the force experienced by the atoms after the sudden turn-on of the potential wells. Atoms optically pumped into the extreme m_F states are accelerated towards the potential minima and vibrate at the frequency characteristic of the potential. The resulting breathing motion at twice the mechanical oscillation frequency produces the modulations in the Bragg scattered intensity shown in Fig. 5. In order to observe these oscillations the rate of optical pumping to the extreme m_F states must be comparable to or higher than the mechanical oscillation frequency. Since the ratio between these quantities is proportional to $\sqrt{I}/|\delta|^3$, the oscillations should be more pronounced at high intensity and small detuning, as observed experimentally. Such oscillations are also seen in 1D experiments and in Monte Carlo calculations.

In this Letter we have presented the first experimental measurements on the time-dependent dynamics of the localization and thermal equilibration of initially disordered atoms in 1D and 3D optical lattices. The results are in good quantitative agreement with 1D Monte Carlo simu-

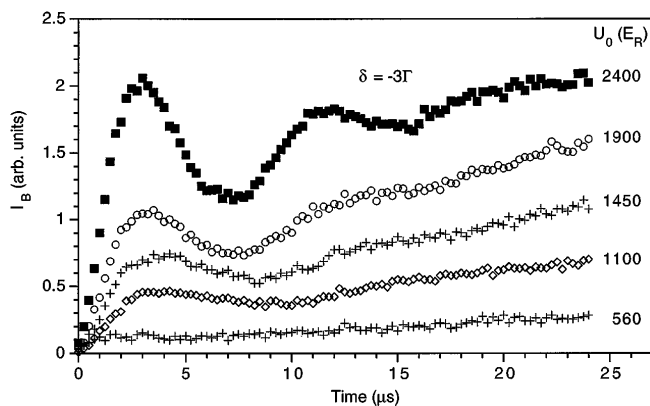


FIG. 5. Short-time behavior of the Bragg intensity in 3D. The lattice detuning is $\delta = -5\Gamma$, except for the uppermost curve which was taken with $\delta = -3\Gamma$. The oscillations reflect a mechanical breathing motion of the atoms in the potential wells.

lations, but some important questions remain unanswered. For example, we do not know why the 3D localization rate is so much slower than the 1D one. Is this related to the existence of orbits with angular momentum in 3D? Does it depend on the axis along which the measurements are made? Furthermore, we do not know whether the cooling process occurs substantially without the movement of an atom from one lattice site to another (local cooling) or if, as in the case of $J = 1/2 \rightarrow J' = 3/2$ cooling, an atom must move from one site to another in order to be cooled. This question could be answered by an experiment sensitive to the time constant for spin flips of the atoms. We hope to study such questions as well as the driven motion of atoms in optical lattices in future research.

This work was partially supported by the U.S. Office of Naval Research and by NSF Grant No. PHY-9312572. G.B. and G.R. acknowledge support by the Alexander-von-Humboldt Foundation.

*Present address: Institut für Quantenoptik, Universität Hannover, Welfengarten 1, D-30167 Hannover, Germany.

†Present address: Stockholm University, Frescativägen 24, S-104 05 Stockholm, Sweden.

- [1] P. Verkerk *et al.*, Phys. Rev. Lett. **68**, 3861 (1992).
- [2] P. S. Jessen *et al.*, Phys. Rev. Lett. **69**, 49 (1992).
- [3] A. Hemmerich and T. W. Hänsch, Phys. Rev. Lett. **70**, 410 (1993).
- [4] G. Birkl, M. Gatzke, I.H. Deutsch, S.L. Rolston, and W.D. Phillips, Phys. Rev. Lett. **75**, 2823 (1995).
- [5] M. Weidemüller *et al.*, Phys. Rev. Lett. **75**, 4583 (1995).
- [6] M.B. Dahan, E. Peik, J. Reichl, Y. Castin, and C. Salomon, Phys. Rev. Lett. **76**, 4508 (1996).
- [7] S.R. Wilkinson, C.F. Bharucha, K.W. Madison, Qian Niu, and M.G. Raizen, Phys. Rev. Lett. **76**, 4512 (1996); Qian Niu, Xian-Geng Zhao, G.A. Georgakis, and M.G. Raizen, Phys. Rev. Lett. **76**, 4504 (1996).
- [8] J. Dalibard and C. Cohen-Tannoudji, J. Opt. Soc. Am. B **11**, 2023 (1989).
- [9] We consider n atoms spatially ordered such that Bragg reflection occurs. The notion of single-atom wave functions is used only as a theoretical tool to find the density matrix of the sample as the average $(1/n) \sum_n |\psi_n\rangle\langle\psi_n|$, using n single-atom wave functions $|\psi_n\rangle$. The validity of this procedure *does not* imply the existence of spatial coherence over many potential wells, as one could conclude from the notion of single-atom wave functions.
- [10] S. Marksteiner, R. Walser, P. Marte, and P. Zoller, Appl. Phys. B **60**, 145 (1995).
- [11] M. Gatzke, G. Birkl, P. S. Jessen, A. Kastberg, S.L. Rolston, and W.D. Phillips (to be published).
- [12] M. Drewsen, Ph. Laurent, A. Nadir, G. Santarelli, A. Clairon, Y. Castin, D. Grison, and C. Salomon, Appl. Phys. B **59**, 283 (1994).
- [13] J. Dalibard, Y. Castin, and K. Mølmer, Phys. Rev. Lett. **68**, 580 (1992).
- [14] K. Mølmer, Y. Castin, and J. Dalibard, J. Opt. Soc. Am. B **10**, 524 (1993).
- [15] Y. Castin, K. Berg-Sørensen, J. Dalibard, and K. Mølmer, Phys. Rev. A **50**, 5092 (1994).